Available online at www.sciencedirect.com
SCIENCE DIRECT®
International Journal of Thermal Sciences 42 (2003) 471–480
International Journal of Thermal Sciences
www.elsevier.com/locate/ijts

Numerical simulation of Rayleigh–Bénard convection in non-Newtonian phase-change-material slurries

Hideo Inaba *, Chuanshan Dai, Akihiko Horibe

Division of Energy Conversion Science, Graduate School of Natural Science and Technology, Okayama University, Tsushimanaka 3-1-1, Okayama 700-8530, Japan

Received 12 December 2001; accepted 18 July 2002

Abstract

A two-dimensional numerical study has been conducted to obtain fluid flow and heat transfer characteristics for Rayleigh–Bénard natural convection of non-Newtonian phase-change-material (PCM) slurries in a rectangular enclosure with isothermal horizontal plates and adiabatic lateral walls. Generally, with the melting of PCM, the slurry's density draws down sharply but continuously and the slurry's specific heat capacity shows a peak value. Some PCM slurries such as microemulsions can exhibit pseudoplastic non-Newtonian fluid behavior. This paper deals with the differences in natural convection and flow patterns between Newtonian and non-Newtonian fluids with or without PCM theoretically. Due to the participation of PCM in natural convection, the dependency of Rayleigh number *Ra* alone cannot reflect its intensity that a modified Stefan number has to be taken into account. A correlation is generalized in the form of $Nu = C \cdot Ra^{l} \cdot Ste^{-m}$ which has a mean deviation of 10.4% in agreement with the calculated data. The numerical simulation has been performed with the following parameters: a shear thinning pseudoplastic fluid for pseudoplastic index $0.8 \leqslant n \leqslant 1.0$, $6 \times 10^3 \leqslant Ra \leqslant 2 \times 10^6$, Prandtl number $Pr = 70$–288, and the aspect ratio of the rectangular enclosure from 10 : 1 to 20 : 1.

Keywords: Natural convection; Phase change material slurry; Numerical; Non-Newtonian fluid; Functionally thermal fluid

1. Introduction

In recent decades, a great deal of attention has been paid to the heat transfer enhancement through the functionally thermal fluids produced by mixing together several distinct components. Microencapsulated phase changing materials (PCM), as an example, have several advantages over traditional single component and single-phase fluids in heat transfer, heat storage and fluid transportation (Inaba and Morita [1], Inaba [2]). Several researchers studied the forced convection in a circular tube to investigate the feasibility of using microencapsulated PCM slurries in district cooling system (Goel et al. [3], Inaba and Morita [4]). Katz [5] and Datta et al. [6,7] conducted studies of natural convection in the PCM fluids and reported that such slurries at low concentration (<5%) could indeed augment heat transfer in natural convection flows. However, besides these researchers there are very few investigations related to the thermal convection in a horizontal layer of these slurries.

The natural convection in a top cooled and bottom heated shallow enclosure, which is known as the Rayleigh–Bénard convection, has been extensively investigated by many researchers over the past four decades for Newtonian Boussinesq fluids since that its simplicity in geometry can be related to many application fields such as a solar energy collector, heat transfer in nuclear reactors, earth's mantle heat transfer, crystal growth from liquid phase, etc. The Rayleigh–Bénard convection also plays an important role in fundamental fluid mechanics and heat transfer study as recently summarized by Getling [8]. A comprehensive review of natural convection in enclosures for Newtonian fluids was made by Ostrach [9]. However, a very few investigations about the thermal convection in non-Newtonian fluids could be available as summarized by Shenoy and Mashelkar [10]. A theoretical research for the natural convection in non-Newtonian PCM slurry in a confined enclosure has not yet been reported to the authors' knowledge. The natural convection problem of heated vertical plate in a PCM slurry (a Newtonian fluid) was theoretically studied

* Corresponding author.
E-mail address: inaba@mech.okayama-u.ac.jp (H. Inaba).

1290-0729/02/$ – see front matter
doi:10.1016/S1290-0729(02)00048-0

Nomenclature

AR	aspect ratio, $= L/H$	t	time ..... s
B	dimensionless term defined in Eq. (7)	T	temperature ..... K
C	coefficient in correlation	u	velocity in horizontal x coordinate ..... $m{\cdot}s^{-1}$
C_p	specific heat ..... $J{\cdot}kg^{-1}{\cdot}K^{-1}$	U	dimensionless velocity in horizontal x coordinate
e	strain rate ..... s^{-1}	v	velocity in vertical y coordinate ..... $m{\cdot}s^{-1}$
g	gravitational constant ..... $m{\cdot}s^{-2}$	V	dimensionless velocity in vertical y coordinate
Gr	Grashof number, $= Ra/Pr$	X, Y	coordinates in dimensionless form
H	height of rectangular enclosure ..... m	x, y	coordinates
h	enthalpy ..... $J{\cdot}kg^{-1}$		
k	thermal conductivity ..... $W{\cdot}m^{-1}{\cdot}K^{-1}$		
K	consistency index of power law model fluids ..... $Pa{\cdot}s^n$		
L	width of rectangular enclosure ..... m		
l	power index of Rayleigh number		
m	power index of Stefan number		
n	pseudoplasticity index of power law model fluids		
Nu	Nusselt number		
P^*	dimensionless pressure		
Pr	Prandtl number, $= K\alpha_0^{n-2}/\rho_0 H^{2n-2}$		
Q	ratio of specific heat capacity, $= C_p/C_{p0}$		
R	ratio of density, $= \rho/\rho_0$		
Ra	Raleigh number, $= \rho_0\beta(T_H - T_C)H^{2n+1}/K\alpha_0^n$		
S_x	dimensionless term defined in Eq. (8)		
S_y	dimensionless term defined in Eq. (9)		

Greek symbols

α	thermal diffusivity	$m^2{\cdot}s^{-1}$
β	volume expansion coefficient	K^{-1}
Θ	dimensionless temperature	
τ	dimensionless time or stress rate	
$\bar{\tau}$	dimensionless stress rate, $= \tau/[K(\alpha_0/H^2)^n]$	
ρ	density	$kg{\cdot}m^{-3}$

Subscript

H	heating plate
C	cooling plate
0	reference state

by Harhira [11]. He observed theoretical enhancements of nearly an order of magnitude in a flow along a vertical flat plate maintained at constant temperature but no experimental data was given to verify the results.

In general, the microencapsulated PCM slurries have complicated physical properties. The interaction between those components in the mixture and the microscopic structural organization of the fluid can manifest their unusual thermophysical and rheological properties owing to phase separation. So far there is no best physical or mathematical model precisely describing the properties of these fluids, which are called complex fluids by some physicists (Daoud and Williams [12]). However, it is reasonable to generalize that a PCM slurry shows a steep descending density and a ascending enthalpy during being heated in the phase change temperature range. A differential scanning calorimetry (DSC) scan can show that there is a peak value corresponding to its maximum latent heat in the temperature range of phase changing. Cooling the fluids makes the density increase. But the density variation with temperature may be different from that of being heated due to the effect of subcooling (Akino et al. [13]). This is ignored in the present work because it would bring more difficulties regarding various different fluids.

Ozoe and Churchill [14] performed the finite difference computation of hydrodynamic stability and thermal convection in power-law and Ellis fluid heated from below for the cases of both rigid and free vertical boundaries. The critical Rayleigh number at which instability sets in was obtained by the extrapolation method of calculated Nusselt number against Rayleigh number. They found that it was difficult to reach a concrete conclusion when they tried to compare their data with the available experimental data obtained by Tsuei [15]. The computation was carried out in a narrow Rayleigh number range for a constant pseudoplastic index n that it was hardly possible to give a comparison of Nusselt number between Newtonian and non-Newtonian fluids or two non-Newtonian fluids with different indexes n at the same defined Rayleigh number. In fact, the natural convection in non-Newtonian fluids has been attracting many geophysicists research interest because of the earth's mantle formation and evolution concerns (Parmentier and Turcotte [16], Christensen [17], Dumoulin et al. [18]), but all their analyses were based on the assumption of infinite Prandtl number ($Pr \to \infty$), and the power law models used were different from ours.

The objective of this paper is to study the influence of phase changing materials on natural convection heat transfer of power law non-Newtonian fluids in an enclosure heated from the bottom and cooled from the top, and to identify the differences of the heat transfer mechanisms between the slurries with PCM and those without PCM. The slurries with a power-law rheology for $0.8 \leqslant n \leqslant 1.0$ have been considered. A two-dimensional approach was used in the present

work, which was easier in dealing with than the 3D simulation and that still as an acceptable method for modeling the 3D flows with at least one homogeneous direction (Kenjereš and Hanjalić [19]). Ostwald–de Waele non-Newtonian fluid model was used in the present numerical analysis.

2. Theoretical model

The present physical model corresponds to a flow regime in a two-dimensional horizontal rectangular cavity of height H and width L. The top and the bottom walls of the cavity are set at a constant temperature of T_C and T_H, respectively. The two sidewalls are adiabatic. The viscosity of the present PCM slurry is assumed to follow the Ostwald–de Waele power law fluid model. The pseudoplastic index n and the consistency viscosity K are assumed to be constant for simplicity in the present numerical computation. However, the pseudoplastic index n and the consistency viscosity K vary generally with temperature and/or concentration. Moreover, the mathematical model is made by considering the following assumptions.

(1) The PCM slurry is homogeneous.
(2) Viscous dissipation is neglected.
(3) For a fluid with PCM, both the density ρ and the specific heat capacity C_p are functions of temperature.

After applying the above-mentioned assumptions, the dimensional governing equations similar to those in Ref. [14] could be obtained. In order to non-dimensionalize those equations, the following dimensionless variables are defined. They are

$$X = \frac{x}{H}, \qquad Y = \frac{y}{H}, \qquad U = \frac{u}{(\alpha_0/H)}$$

$$V = \frac{v}{(\alpha_0/H)}, \qquad \Theta = \frac{T - T_C}{T_H - T_C}, \qquad \tau = \frac{t}{(H^2/\alpha_0)}$$

$$P^* = \frac{p}{(\rho_0\alpha_0^2/H^2)}, \qquad R = \frac{\rho}{\rho_0}, \qquad Q = \frac{C_p}{C_{p0}}$$

By introducing these non-dimensional variables, the non-dimensionalized deviatoric stress rate for Ostwald–de Waele power law fluids can be expressed as

$$\bar{\tau}_{ij} = -\left\{2\left[\left(\frac{\partial U}{\partial X}\right)^2 + \left(\frac{\partial V}{\partial Y}\right)^2\right] + \left(\frac{\partial V}{\partial X} + \frac{\partial U}{\partial Y}\right)^2\right\}^{(n-1)/2} 2\bar{e}_{ij} \tag{1}$$

where $\bar{e}_{ij}$ is the non-dimensional strain rate tensor based on the reference [16].

The non-dimensionalized governing equations are as follows.

Continuity:

$$\frac{\partial R}{\partial \tau} + \frac{\partial (RU)}{\partial X} + \frac{\partial (RV)}{\partial Y} = 0 \tag{2}$$

Momentum:

$$\frac{\partial (RU)}{\partial \tau} + \frac{\partial (RUU)}{\partial X} + \frac{\partial (RUV)}{\partial Y} = -\frac{\partial P^*}{\partial X} + Pr\left(\frac{\partial}{\partial X}\left(B\frac{\partial U}{\partial X}\right) + \frac{\partial}{\partial Y}\left(B\frac{\partial U}{\partial Y}\right) + S_X\right) \tag{3}$$

$$\frac{\partial (RV)}{\partial \tau} + \frac{\partial (RUV)}{\partial X} + \frac{\partial (RVV)}{\partial Y} = -\frac{\partial P^*}{\partial Y} + Ra\,Pr\,\Theta + Pr\left(\frac{\partial}{\partial X}\left(B\frac{\partial V}{\partial X}\right) + \frac{\partial}{\partial Y}\left(B\frac{\partial V}{\partial Y}\right) + S_Y\right) \tag{4}$$

Energy:

$$\frac{\partial (RQ\Theta)}{\partial \tau} + \frac{\partial (RQU\Theta)}{\partial X} + \frac{\partial (RQV\Theta)}{\partial Y} = \frac{\partial^2 \Theta}{\partial X^2} + \frac{\partial^2 \Theta}{\partial Y^2} \tag{5}$$

where, each non-dimensional variable is defined as follows:

Prandtl number:

$$Pr = \frac{K\alpha_0^{n-2}}{\rho_0 H^{2n-2}} \tag{6}$$

Rayleigh number:

$$Ra = \frac{\rho_0 g\beta(T_H - T_C)H^{2n+1}}{K\alpha_0^n} \tag{7}$$

$$B = \left\{2\left[\left(\frac{\partial U}{\partial X}\right)^2 + \left(\frac{\partial V}{\partial Y}\right)^2\right] + \left(\frac{\partial U}{\partial Y} + \frac{\partial V}{\partial X}\right)^2\right\}^{(n-1)/2} \tag{8}$$

$$S_X = \frac{\partial}{\partial X}\left(B\frac{\partial U}{\partial X}\right) + \frac{\partial}{\partial Y}\left(B\frac{\partial V}{\partial X}\right) \tag{9}$$

$$S_Y = \frac{\partial}{\partial X}\left(B\frac{\partial U}{\partial Y}\right) + \frac{\partial}{\partial Y}\left(B\frac{\partial V}{\partial Y}\right) \tag{10}$$

The boundary conditions are:

$$U(\tau, 0, Y) = U(\tau, L/H, Y) = U(\tau, X, 0) = U(\tau, X, 1) = 0 \tag{11}$$

$$V(\tau, 0, Y) = V(\tau, L/H, Y) = V(\tau, X, 0) = V(\tau, X, 1) = 0 \tag{12}$$

$$\Theta(\tau, X, 0) = 1 \tag{13}$$

$$\Theta(\tau, X, 1) = 0 \tag{14}$$

$$\frac{\partial \Theta}{\partial X}(\tau, 0, Y) = \frac{\partial \Theta}{\partial X}(\tau, L/H, Y) = 0 \tag{15}$$

The initial conditions are:

$$U(0, X, Y) = V(0, X, Y) = \Theta(0, X, Y) = 0 \tag{16}$$

R and Q in the above equations are the ratios of density and specific heat capacity to their reference points, respectively. The specific heat capacity C_p is considered to be a constant for a fluid without PCM and a variable changing with temperature for a PCM slurry. They were obtained by fitting the measured data of an Oil/Water type

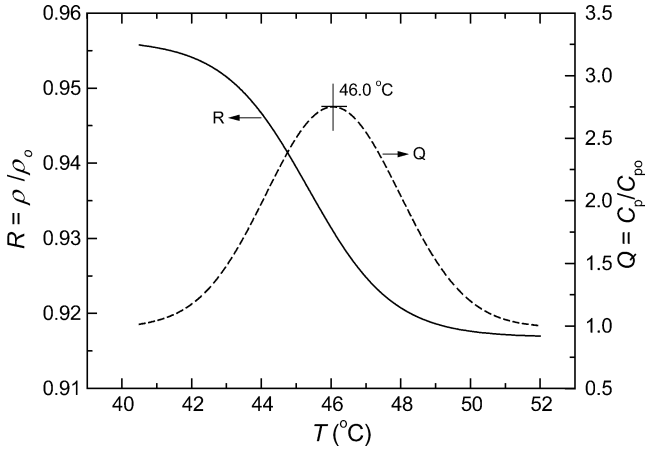

Fig. 1. Dimensionless density and specific heat capacity used in simulation.

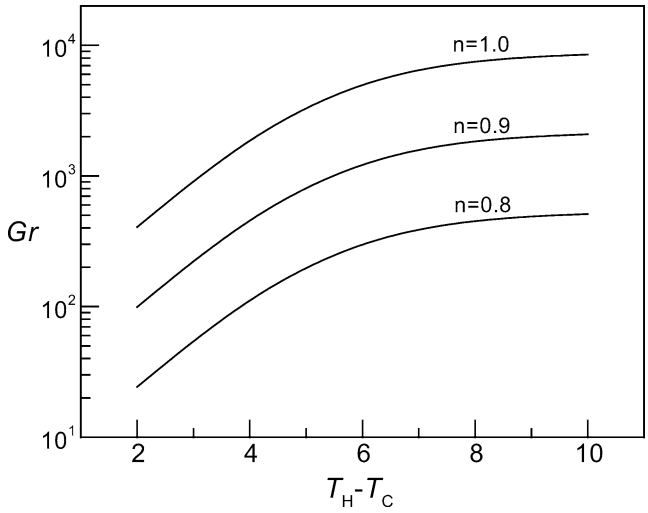

Fig. 2. The input Grashof numbers depending on the temperature difference and the pseudoplasticity index n for enclosure $H = 12$ mm, $L = 120$ mm or aspect ratio 10 : 1.

microemulsion slurry, which has a 30% mass concentration of paraffin, 5% of surfactant and 65% of water. Both the results of differential scanning calorimetry(DSC) scan and direct density measurement showed that it has a peak in latent heat at temperature about 45.3 °C. The reference point ρ_0 is chosen as unit and C_{p0} as the specific heat capacity at 40 °C the maximum temperature while the PCM is in single solid phase in the slurry. So that R and Q can be expressed in the following equations and as shown in Fig. 1.
Ratio of density:

$$R = 0.9168 + \frac{0.03957}{1 + e^{(T-45.4)/1.19}} \tag{17}$$

Ratio of specific heat capacity:

$$Q = 0.9895 + 1.782e^{-0.14(T-46.0)^2} \tag{18}$$

Another parameter that should be mentioned is the modified Stefan number. It is not a direct input data, but an important parameter to be used for correlating the calculated results later. Because the phase change process happens continuously in a temperature range rather than at a fixed temperature, a modified *Ste* number is defined as

$$Ste = \frac{T_H - T_C}{\int_{T_C}^{T_H} Q \,\mathrm{d}T} \tag{19}$$

3. Numerical method and input data sheet

The governing equations were solved in a uniform, two-dimensional staggered grid based on the control volume method (Patankar [20]). The SIMPLE algorithm was used to solve the coupled heat transfer and fluid flow problem. The central-difference schemes were applied for all diffusive terms and the power law scheme for the convective terms. Time stepping was done by an implicit Backward–Euler scheme. For non-Newtonian fluids the smaller time step is necessary to get a convergent solution. The time step $\Delta\tau$ was generally 2×10^{-5} for the unsteady calculations and 2×10^{-4} or 1×10^{-3} when only the final steady-state solution was required. The grids were uniformly given with 400×20, 200×20 for the cases of aspect ratio of 20 : 1, 10 : 1, respectively, so that in any cases the control volume sizes were always $\Delta X = \Delta Y = 0.05$.

The input parameter set of Grashof number Gr and Prandtl number Pr was based on the correlated density function with temperature of Eq. (11). An arithmetic mean density with temperature was used in deriving the thermal diffusivity. In order that $\Theta = 0$ and $\Theta = 1$ are always referred to the cooling and heating plate temperatures, respectively, the values of Eqs. (17) and (18) should correspondingly be varied with the cooling plate temperature T_C and/or heating plate temperature T_H. Since Prandtl number does not vary much with temperature we took it as a constant at a specific pseudoplasticity index n. The input Grashof numbers depending on the temperature difference and the pseudoplasticity index n at a specific height of enclosure are shown in Fig. 2.

4. Validation

The present code was firstly verified for natural convection in a Newtonian fluid in a sidewall heated and a sidewall cooled square cavity problem. In order to make a comparison with the results obtained by de Vahl Davis and Jones [21], the boundary conditions of equations (12)–(14) in the numerical computation have to be replaced by

$$\Theta(\tau, 0, Y) = 1.0 \tag{20}$$

$$\Theta(\tau, 1, Y) = 0.0 \tag{21}$$

$$\frac{\partial \Theta}{\partial Y}(\tau, X, 0) = \frac{\partial \Theta}{\partial Y}(\tau, X, 1) = 0 \tag{22}$$

The numerical computations were performed on uniform grids of 20×20, 40×40 and 60×60, respectively. The

average Nusselt number obtained are 2.293, 2.259 and 2.251, respectively, for $Pr = 10$ and $Ra = 10^4$. These values of Nusselt number coincide well with that obtained by de Vahl Davis and Jones [21]. A grid independence test has been also performed for a Rayleigh–Bénard configuration with an aspect ratio of $AR = 10 : 1$ at $Pr = 6$, $Ra = 10^4$ with uniform grids of 200×10, 200×20, 200×40 and 200×60. The Nusselt numbers obtained are 2.374, 2.439, 2.462 and 2.471, respectively, from a coarse to a fine grid. By using the correlation recommended by Hollands et al. [22], which is for two infinite horizontal plates configuration, the Nusselt number calculated is 2.399. As a compromise between computing time and accuracy, the 200×20 grid is chosen for most of the present computations.

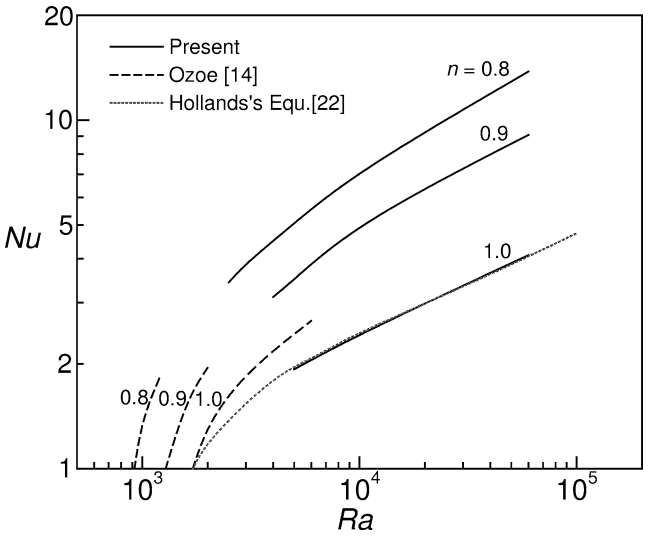

Fig. 3. Comparison of computed results with the correlation of Hollands et al. [22] and the theoretical results of Ozoe et al. [14].

For the verification of natural convection in a non-Newtonian fluid, the numerical result obtained by stream function method (Ozoe and Churchill [14]) was taken as a reference in the present study. The present numerical results are shown in Fig. 3 together with the correlation curve of Hollands et al. [22]. For the Newtonian fluid ($n = 1$), the present calculated results are within 5% in deviation in agreement with those of Hollands et al. For the non-Newtonian fluid ($n < 1$), the present calculated data seem to fit the curve extrapolated from those of Ozoe and Churchill [14]. Fig. 4 shows the streamlines and isotherms for a Newtonian fluid ($n = 1$) and a non-Newtonian fluid ($n = 0.8$) for $AR = 10$, $Ra = 10^4$ and $Pr = 10$. It can be seen that the decrease in pseudoplastic index n results in an increase in Nusselt number. This can be explained by the fact that the fluid flow could be changed more locally for a pseudoplastic shear thinning fluid since a larger strain rate always corresponds to a less effective viscosity for $n < 1$.

The experimental validation was also conducted for a natural convection in an enclosure of $120 \times 120 \times 8.3$. A brief introduction about the experimental apparatus is given as follows. The schematic diagram of experimental apparatus is shown in Fig. 5. The rectangular enclosure consisted of a transparent acrylic supporter (10 mm thick) and two copper plates (10 mm thick). The copper plates were mounted to the top and bottom ends of the supporter, respectively. The temperature of the top cooling copper plate was maintained by circulating the cooling brine through

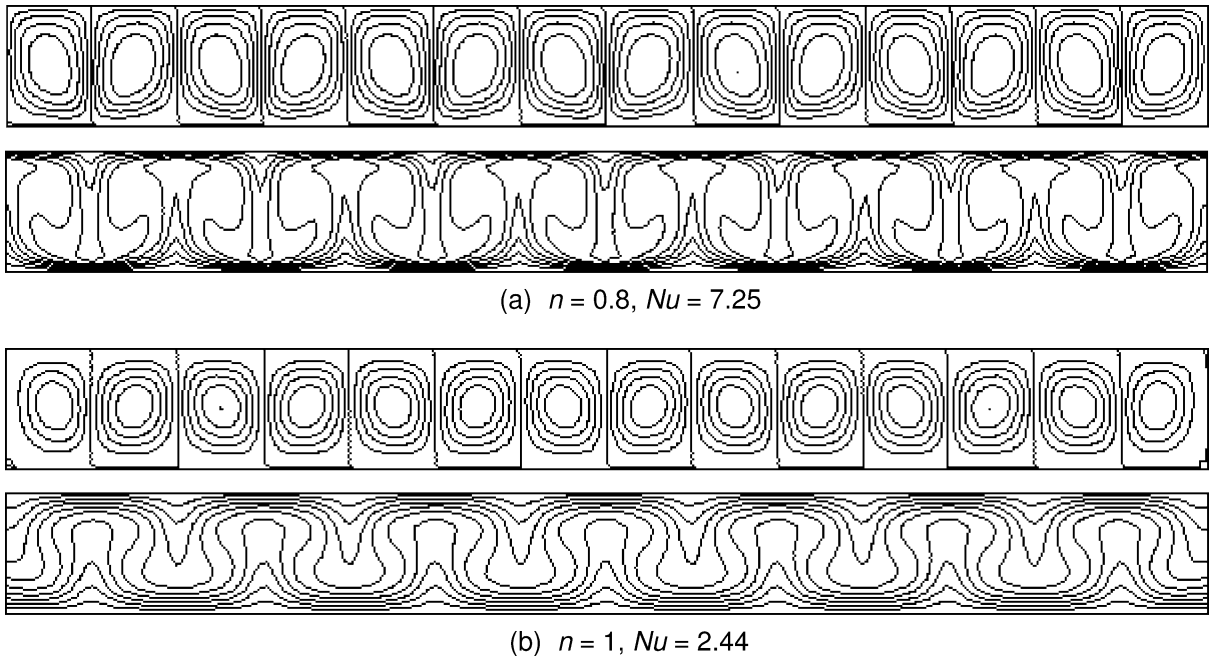

Fig. 4. Streamlines (top) and isotherms (bottom) of pseudoplastic power law non-Newtonian fluids (a) and Newtonian fluids (b) for enclosure $AR = 10$, $Ra = 10000$ and $Pr = 10$.

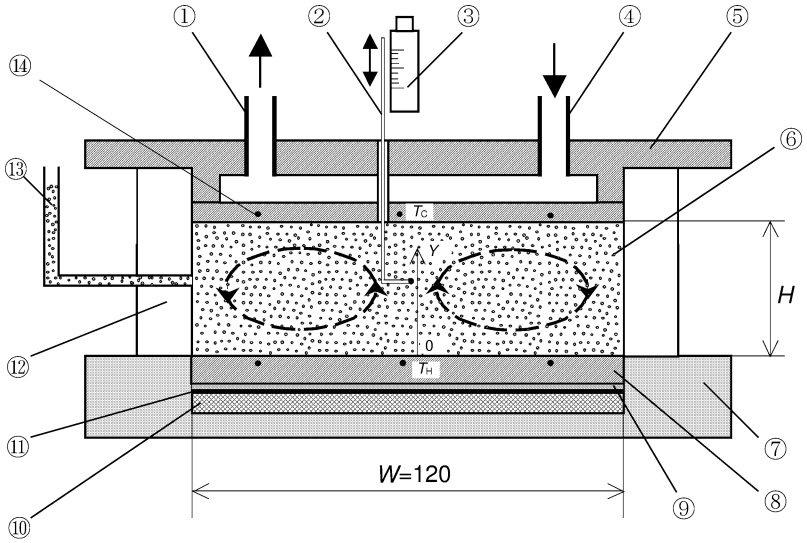

Fig. 5. Schematic of experimental apparatus.

a water bath. A 0.7 mm thick electric film heater was arranged below the bottom of the lower heating copper plate. A 0.2 mm thick and 50 mm in square film heat flux sensor was placed between the heating copper plate and the film heater, which has the measuring accuracy of 1.0 $W \cdot m^2$. The backside of the film heater was covered with 5 mm thick foamed thermal insulating material and a 15 mm thick bakelite plate. The whole test section was wrapped with 50 mm thick foamed thermal insulating material. A glass pipe of 8.0 mm in inner diameter was placed vertically connecting to the test section as an expansion reservoir of the testing fluid. The average temperatures of the heating and cooling copper plates were measured through six 0.1 mm in diameter Cu–Co thermocouples, and two of the six thermocouples were buried in the middle and the others were located around the heating or the cooling plate. The temperature of the heating copper plate were adjusted by controlling the input electric power of the heater. Two T-type thermocouples supported by a 1.06 mm in an outer diameter and 0.18 mm thick stainless pipe, which could be traversed in the vertical direction, was installed to measure the vertical fluid temperature distribution in the center of the enclosure and, its position was measured by a micrometer. The experimental apparatus was calibrated by turning it upside down and performing temperature steady conductive experiment by using the distilled water. A water solution with 200 ppm Cetyltrimethylammonium

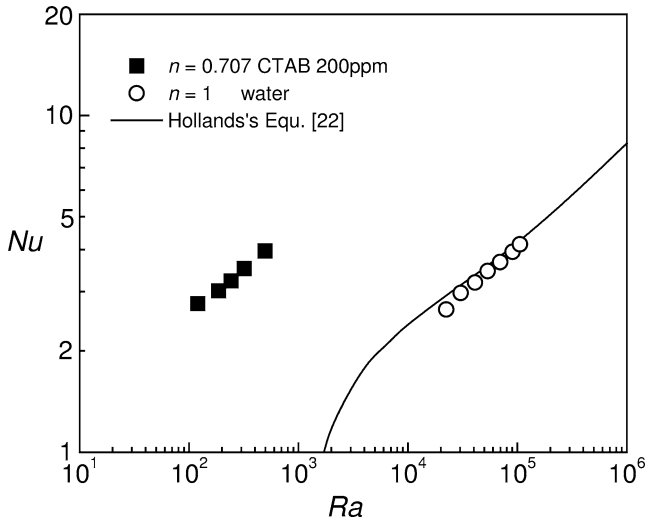

Fig. 6. Experimental test of water (open circle) and CTAB solution (solid square) in an enclosure of 120 × 120 × 8.3.

Bromide (CTAB) was used as a power law non-Newtonian fluid ($n = 0.707$). The data of the water CTAB solution were plotted in the smaller region of Rayleigh number due to its high effective viscosity. As shown in Fig. 6, the extrapolated *Nu–Ra* curve seems to be in quantitatively agreement with the results obtained by the present numerical computation.

5. Results and discussion

In order to get an understanding of the effect of PCM in fluids on natural convection, the numerical simulation is performed in a way that one fluid (without PCM) varies only in density with temperature. The specific heat capacity is given as a constant. The other fluid (with PCM) varies both in density and in specific heat capacity. A comparison has been made between these two fluids. The imposed boundary conditions are that the cooling plate temperature is fixed at 40 °C and the heating plate temperature is varied from 42 °C to 54 °C with an increasing step of 2 °C. The input Rayleigh numbers and Prandtl numbers are the same for both cases as long as their boundary conditions are the same. To minimize the sidewall effect, two kinds of enclosures with a large aspect ratio of 10 : 1 and 20 : 1 are chosen. The pseudoplastic fluid indexes n are 0.8, 0.9 and 1.0, respectively. It is unrealistic to reach the results for all possible combinations of these parameters. The later discussion is based on the results within the above parameter ranges.

5.1. Effect of PCM

Fig. 7 shows the computed results for the natural convection in Newtonian fluids with and without PCM for the enclosure with the aspect ratio of $AR = 10$. By comparing with the fluids without PCM, higher Nusselt numbers have been observed for the fluids with PCM in the phase changing temperature range. The maximum Nusselt number for the fluid with PCM approximately corresponds to the heating plate temperature of 46 °C. Because the density variation decreases after 50 °C, the trend of the Nusselt number variation with *Ra* cannot be seen clearly even the heating plate is given as high as 54 °C. Therefore, as an extension in numerical simulation for this configuration, the input Rayleigh number is given as high as 8.0×10^5, which corresponds approximately to the heating plate temperature of 92 °C on the assumption that the volumetric thermal expansion coefficient β is constant in the liquid phase and equals to the average of from 50 °C to 52 °C. It is shown in Fig. 7 that the Nusselt number restores increasing again after a short drop down. The heat transfer coefficients can be obtained by giving the arithmetic mean thermal conductivity, which decreases slightly with an increase in temperature in the phase change temperature range due to a volumetric expansion. They are plotted in Fig. 8, which show that the fluids with PCM have higher heat transfer coefficients than those without PCM in natural convection at the same boundary conditions. As aforementioned above, the heat transfer coefficient reaches a maximum value at a heating plate temperature of about 48 °C, which is near the temperature that the specific heat capacity of the PCM slurry has its peak value. This could be explained as follows. The melting process near the heating plate could maintain the heat being transferred in a high temperature difference, and in turn a larger heat flux can be obtained compared with the fluids

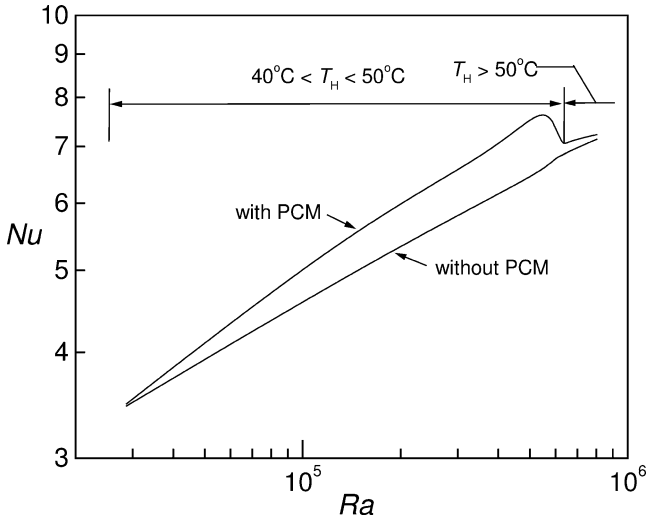

Fig. 7. Calculated *Nu* vs. *Ra* for Newtonian fluids with PCM and for enclosure $AR = 10$.

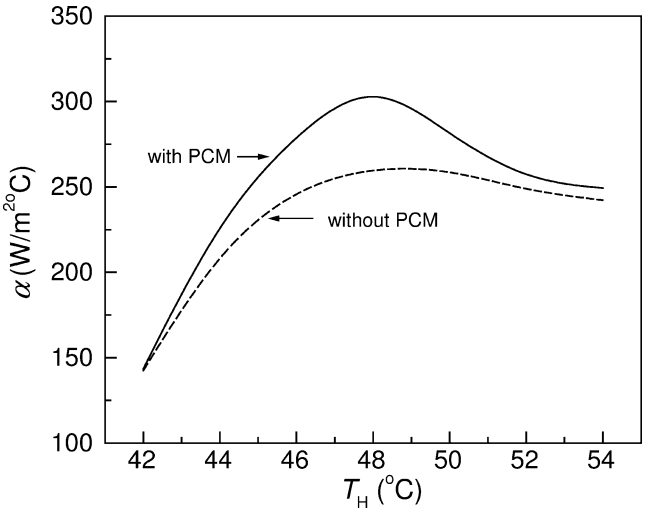

Fig. 8. Calculated heat transfer coefficients vs. the bottom plate temperature for Newtonian fluids with (solid) and without (dash) PCM and for enclosure $AR = 10$ and $T_C = 40$ °C.

without PCM. As pointed out by Datta et al. [7], the phase changing process near the heating and cooling plates causes an increase in the heat transfer. Although phase changing process also happens in the ascending and descending plumes of the fluid, the phase changing process near the horizontal boundaries plays a key role in heat transfer enhancement. When the heating plate temperature is above 50 °C all the phase changing materials in the fluid have been changed into liquid phase upon reaching the heating plate, so that the enhancement of heat transfer is minimized. It will be very time consuming on considering both boundary temperatures are to be varied. In the present numerical simulation the cooling plate temperature is kept at 40 °C, which is considered to be the maximum temperature for PCM in solid phase. If the cooling plate is also maintained at a temperature in a phase changing range, the heat transfer performance

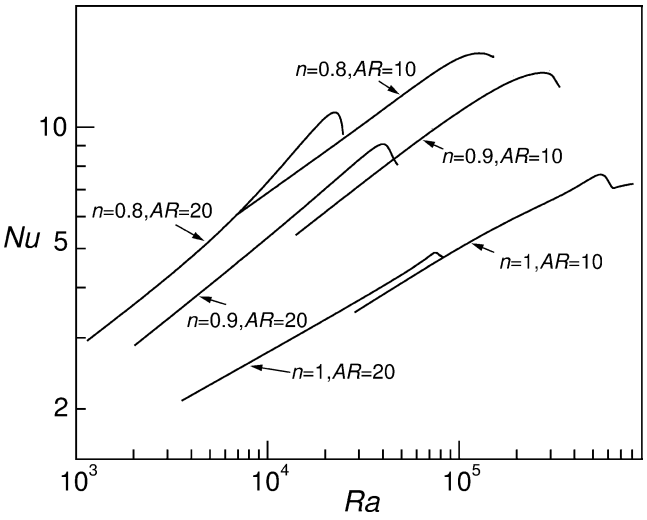

Fig. 9. Calculated *Nu* vs. *Ra* for pseudoplastic fluids ($n = 1.0$, 0.9 and 0.8) with PCM for enclosures $AR = 10$ and 20.

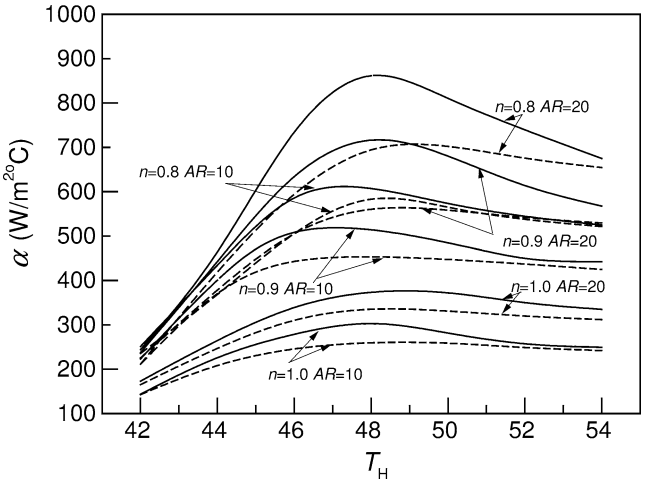

Fig. 10. Calculated heat transfer coefficients vs. the bottom plate temperature for pseudoplastic fluids ($n = 1.0$, 0.9 and 0.8) with (solid) and without (dash) PCM for enclosures $AR = 10$ and 20, $T_C = 40\,^{\circ}\mathrm{C}$.

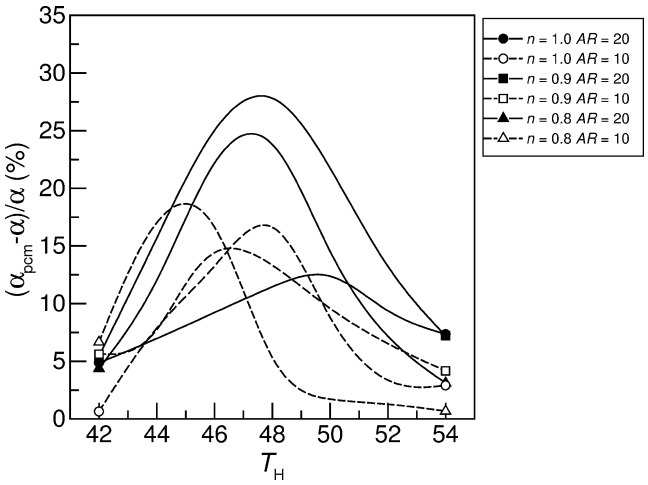

Fig. 11. Percentages of increment of heat transfer coefficient for the fluids with PCM compared with those of without PCM.

can be improved further because the mechanism is applicable for both the heating plate and the cooling plate.

5.2. Effect of pseudoplastic index and aspect ratio

Fig. 9 shows the relationship between the Nusselt number and the Rayleigh number in non-Newtonian fluids for pseudoplastic indexes of 0.8, 0.9 and enclosures with the aspect ratios of 10 : 1 and 20 : 1. The result of in Newtonian fluids is also shown in the figure. The peak values correspond to the heating plate temperature near about 46 °C, which is consistent with the temperature having the maximum specific capacity. The natural convections in the fluids with and without PCM for each configuration are calculated simultaneously for a comparison. The variation in heat transfer coefficients with the heating plate temperature T_H ($T_C = 40\,^{\circ}\mathrm{C}$) for both fluids are shown in Fig. 10. The dash lines in Fig. 10 are the results of natural convection in fluids without PCM. As noted above, the fluids with PCM have higher Nusselt numbers or heat transfer coefficients than those without PCM in natural convection. A smaller pseudoplastic fluid index n results in a higher heat transfer coefficient for the configuration. The enclosure of $AR = 10$ has a lower heat transfer coefficient as compared with the enclosure of $AR = 20$ at a same pseudoplastic fluid index n. The heat transfer enhancement due to PCM is minimized for an enclosure with $AR = 10$ or a higher dimension enclosure. This can be explained as that the input Prandtl number Pr increases with decreasing enclosure height H and pseudoplastic index number n according to Eq. (6). The percentages of increment of heat transfer coefficient for the fluids with PCM compared with those of without PCM are shown in Fig. 11. It can be seen that the increments have peak values for all of these configurations, and the maximum points do not exactly correspond to the heating plate temperature of 46.0 °C but scatter about between 44 °C and 50 °C. This is probably resulted from the nonlinearity of the coupled heat and mass problem or some other reasons that not very clear for us.

5.3. A correlation of calculated results

As shown in Figs. 7 and 9, for natural convection in a PCM slurry, the increasing of Rayleigh number cannot guarantee an increase in Nusselt number. The phase changing process has to be taken into an account. This indicates that the only dependence of Rayleigh number defined in the present paper cannot reflect the intensity of natural convection for the fluids with PCM. Some other parameters, which can evaluate the effect of phase changing process on heat transfer, have to be included. The authors argue that the heat transfer enhancement due to the participation of PCM is proportional to the term of $\Delta h/[C_{p0}(T_H - T_C)]$. Where Δh is the enthalpy increment of the PCM slurry from the cooling temperature T_C to the heating temperature T_H. This term is

equal to unit for fluids having no PCM. The expression of $\Delta h/(T_H - T_C)$ is a quite familiar term, which is just the definition of specific heat capacity if the temperature difference $(T_H - T_C)$ is infinitesimal. Generally, the enthalpy Δh cannot be differentiated respect to temperature at melting point for a material with first-order phase transition such as ice. It seems to be, however, applicable to a microemulsion PCM slurry. Therefore, a modified Stefan number defined in Eq. (19) is proposed for correlating the calculated data. In our correlation, the Prandtl number *Pr* and aspect ratio *AR* have not been considered, since the two parameters are not independent for a non-Newtonian fluids (Rohsenow et al. [23]). The generalized correlation based on our calculated data can be expressed as follows.

$$Nu = (1.1 - 0.78n)Ra^{1/(3.5n+1)}\,Ste^{-(1.9-1.65n)} \tag{23}$$

It can be concluded that the power index of Rayleigh number increases with a decrease in pseudoplastic index number n. The exponent of Rayleigh number is located in between $1/(3n+2)$ and $1/(3n+1)$, the values, respectively, suggested by Dale and Emery [24], Reilly et al. [25] in an experimental correlation for a free convection in non-Newtonian fluids from a heated vertical plate. The authors also noted that the product of $Gr \cdot Pr^n$ with their definitions in [24] is exactly the simply form of *Ra* defined in our paper. Because the exponent of the Stefan number is negative, the Nusselt number increases as the pseudoplastic index number n decreases ($Ste \leqslant 1$). As a consequence, a smaller Stefan number corresponds to a higher Nusselt number, which is consistent with the computed results of Harhira [11] for a free convection from a vertical plate problem. When the Stefan number is equal to unit, it means that no phase changing occurs in natural convection. As a result, the Nusselt number becomes a function of the Rayleigh number only. The average deviation for the generalized correlation is 10.4% in agreement with the calculated data.

6. Summary

This paper has elucidated that PCM slurries could enhance the natural convection heat transfer in enclosures on considering that the fluids have a continuous variation in density and enthalpy with temperature. It could be seen that the enhancement is closely related to the specific heat capacities at the temperatures of bottom heating and top cooling plates. By comparing with those of fluids without PCM, the maximum enhancement in heat transfer could be up to 30% for the given density and specific heat capacity functions and configurations in the paper. When the cooling plate temperature was set to 40 °C, the maximum heat transfer coefficients could be reached if the bottom heating plate temperature was controlled at about 46 °C, at which the slurry has its maximum specific heat capacity. It could be conjectured that further heat transfer enhancement could be obtained by setting the cooling plate temperature also near 46 °C. Because, the heat transfer mechanism is applicable to both heating plate and cooling plate.

Rayleigh number, Prandtl number and aspect ratio could be the main dependencies for evaluating a natural convection in enclosures for most of Newtonian and non-Newtonian fluids. Those will, however, become inadequate, or some modifications will be necessary for evaluating the natural convection in a PCM slurry. A modified Stefan number, therefore, defined in the paper has been proved to be a good dependency on correlating the calculated data in our work. However, for the concern of that the natural convection in the phase changing temperature range strongly invalidates the Boussinesq assumption, as pointed out earlier, the verification of these results is still essential for the problem, which is left as an open question for the future work.

References

[1] H. Inaba, S. Morita, Cold heat-release characteristics of phase-change by air–emulsion direct-contact heat exchange method, Internat. J. Heat Mass Transfer 39 (9) (1995) 1797–1803.
[2] H. Inaba, New challenge in advanced thermal energy transportation using functionally thermal fluids, Internat. J. Thermal Sci. 39 (2000) 991–1003.
[3] M. Goel, S.K. Roy, S. Sengupta, Laminar forced convection heat transfer in microcapsulated phase change material suspensions, Internat. J. Heat Mass Transfer 37 (4) (1994) 593–604.
[4] H. Inaba, S. Morita, Flow and cold heat-storage characteristics of phase-change emulsion in a coiled double-tube heat exchanger, ASME J. Heat Transfer 117 (1995) 440–446.
[5] L. Katz, Natural convection heat transfer with fluids using particles while undergoing phase change, Ph.D. Dissertation, Department of Mechanical Engineering; Massachusetts Institute of Technology, Massachusetts, 1968.
[6] P. Datta, S. Sengupta, S.K. Roy, Natural convection heat transfer in an enclosure with suspensions of microcapsulated phase change materials, ASME General Papers in Heat Transfer, HTD 204 (1992) 133–144.
[7] P. Datta, S. Sengupta, T. Singh, Raleigh and Prandtl number effects in natural convection in enclosures with microencapsulated phase change materials slurries, in: Symposium on 33rd Heat Transfer in Japan, 1996, pp. 225–226.
[8] A.V. Getling, Rayleigh–Bénard Convection: Structures and Dynamics, in: Advanced Series in Nonlinear Dynamics, Vol. 11, World Scientific, Singapore, 1998.
[9] S. Ostrach, Natural convection in enclosures, ASME J. Heat Transfer 110 (1988) 1175–1190.
[10] A.V. Shenoy, R.A. Mashelkar, Thermal convection in non-Newtonian fluids, Adv. Heat Transfer 15 (1982).
[11] M. Harhira, Natural convection heat transfer of microencapsulated phase change material suspensions past a vertical flat plate, M.S. Thesis, Mechanical Engineering, University of Miami, 1992.
[12] M. Daoud, C.E. Williams, Soft Matter Physics, Springer-Verlag, Berlin, 1999.
[13] N. Akino, K. Takase, Y. Okada, Microencapsulated PCM slurry for heat transfer media (2) effect of particle diameter on phase behavior, in: Symposium on 31st Heat Transfer in Japan, 1994, pp. 589–591.
[14] H. Ozoe, S.W. Churchill, Hydrodynamic stability and natural convection in Ostwald–de Waele and Ellis fluids: The development of a numerical solution, AIChE J. 18 (6) (1972) 1196–1206.
[15] H.S. Tsuei, Thermal instability and heat transport of a layer of non-Newtonian fluid, Ph.D. Thesis, Syracuse University, New York, 1970.

[16] E.M. Parmentier, D.L. Turcotte, Studies of finite amplitude non-Newtonian thermal convection with application to convection in the earth mantle, J. Geophys. Res. 81 (11) (1976) 1839–1946.
[17] U. Christensen, Convection in a variable-viscosity fluid: Newtonian versus power-law rheology, Earth Planetary Sci. Lett. 64 (1983) 153–162.
[18] C. Dumoulin, M.P. Doin, L. Fleitout, Heat transport in stagnant lid convection with temperature- and pressure-dependent Newtonian or non-Newtonian rheology, J. Geophys. Res. 104 (6) B6 (1999) 12759–12777.
[19] S. Kenjereš, K. Hanjalić, Convective rolls and heat transfer in finite-length Rayleigh–Bénard convection: A two-dimensional numerical study, Phys. Rev. E 62 (6) (2000) 7987–7998.
[20] S.V. Patankar, Numerical Heat Transfer and Fluid Flow, Hemisphere, New York, 1980.
[21] G. de Vahl Davis, I.P. Jones, Natural convection in a square cavity: A comparison exercise, Internat. J. Numer. Meth. Fluids 3 (1983) 227–248.
[22] K.G.T. Hollands, G.D. Raithby, L. Konicek, Correlation equation for free convection heat transfer in horizontal layers of air and water, Internat. J. Heat Mass Transfer 18 (1975) 879–884.
[23] W.M. Rohsenow, J.P. Hartnett, E.N. Ganic, Handbook of Heat Transfer Fundamentals, 2nd Edition, McGraw-Hill, New York, 1985, Chapter 6.
[24] J.D. Dale, A.F. Emery, The Free convection of heat from a vertical plate to several non-Newtonian “pseudoplastic fluid”, ASME J. Heat Transfer 94 (1972) 64–72.
[25] I.G. Reilly, C. Tien, M. Adelman, Experimental study of natural convection heat transfer from a vertical plate in non-Newtonian fluid, Canad. J. Chem. Engrg. (1965) 157–160.